

DELFT UNIVERSITY OF TECHNOLOGY

SPECTRAL DOMAIN METHODS IN ELECTROMAGNETICS  
EE4620

---

## Assignment 4: Leaky Wave Antennas

---

*Authors:*  
Cagin Sari(5545404)

June 25, 2023



# 1 Question 1: Superstrate Analysis

In this question, the propagation constant and far-field of the superstrate antenna geometry are analysed also with the directivity and bandwidth.

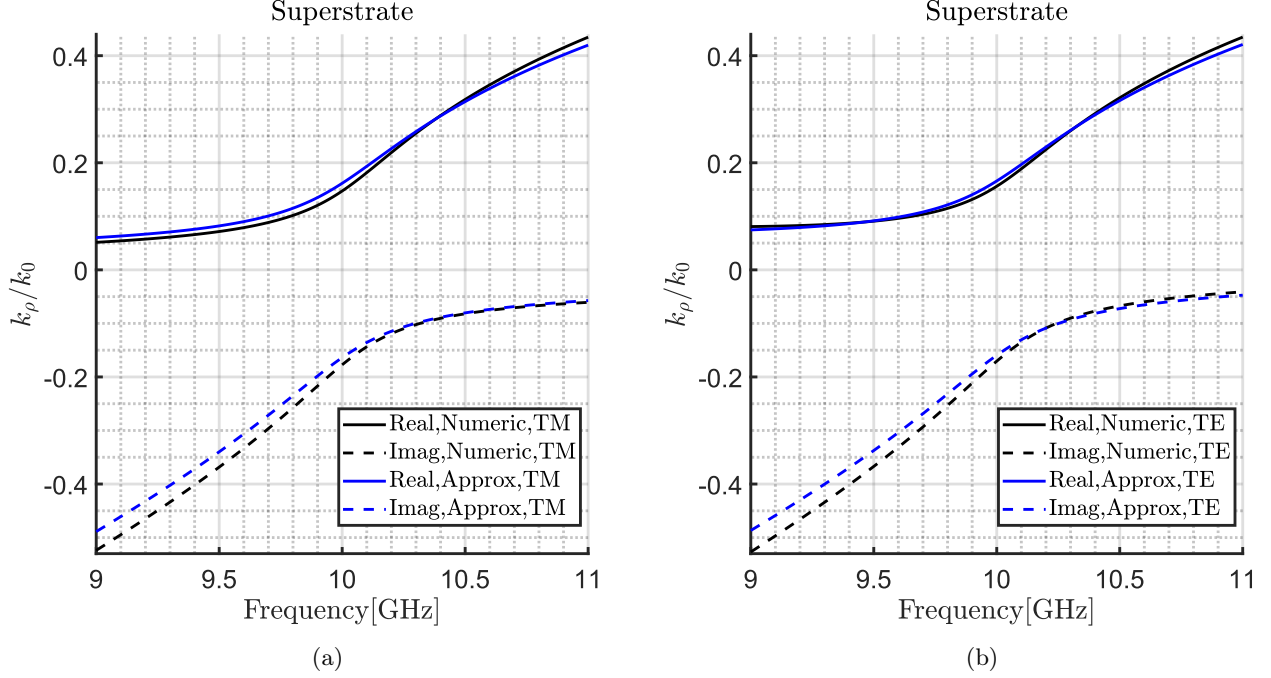


Figure 1: The change in propagation constant with frequency ( $\epsilon_r=12$ ), where 6a TM and 6b TE

The analytical and numeric values of the propagation constant are very close, this can also be seen from the figure 1. Another observation is unlike in the surface waves assignment (Assignment 3) the TM and TE modes propagate around the same frequencies.

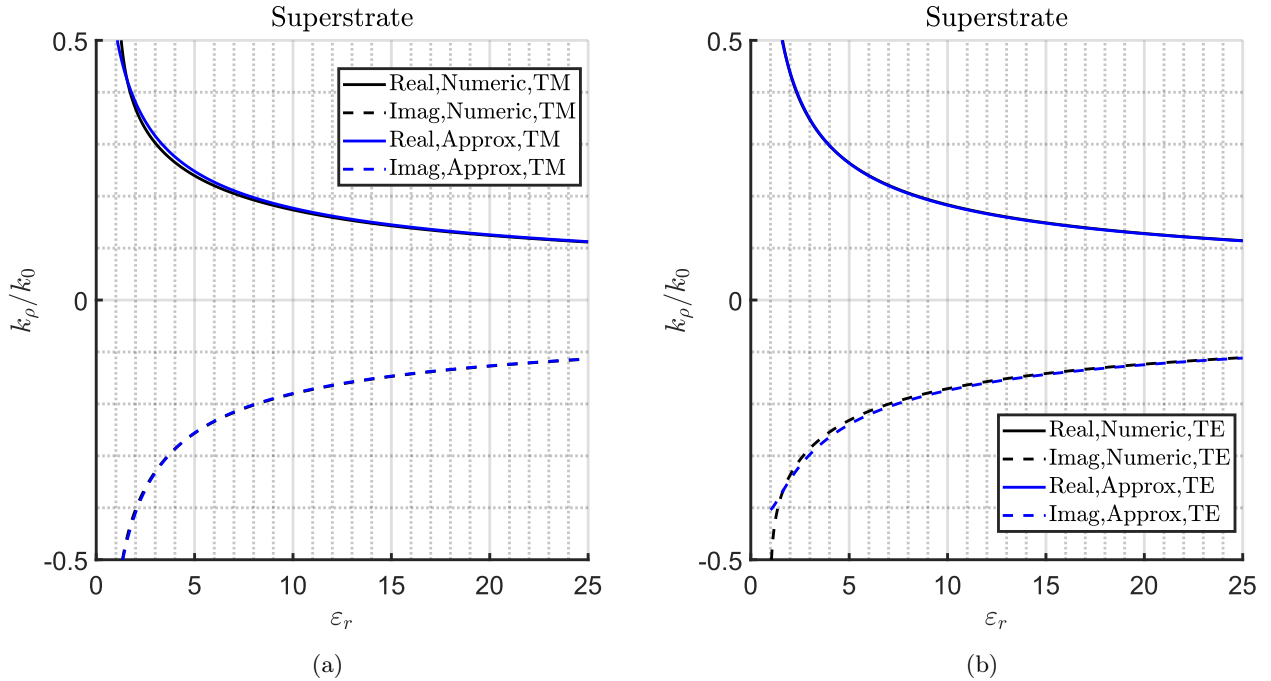


Figure 2: The change in propagation constant with relative permittivity (frequency=11 GHz), where 6a TM and 6b TE

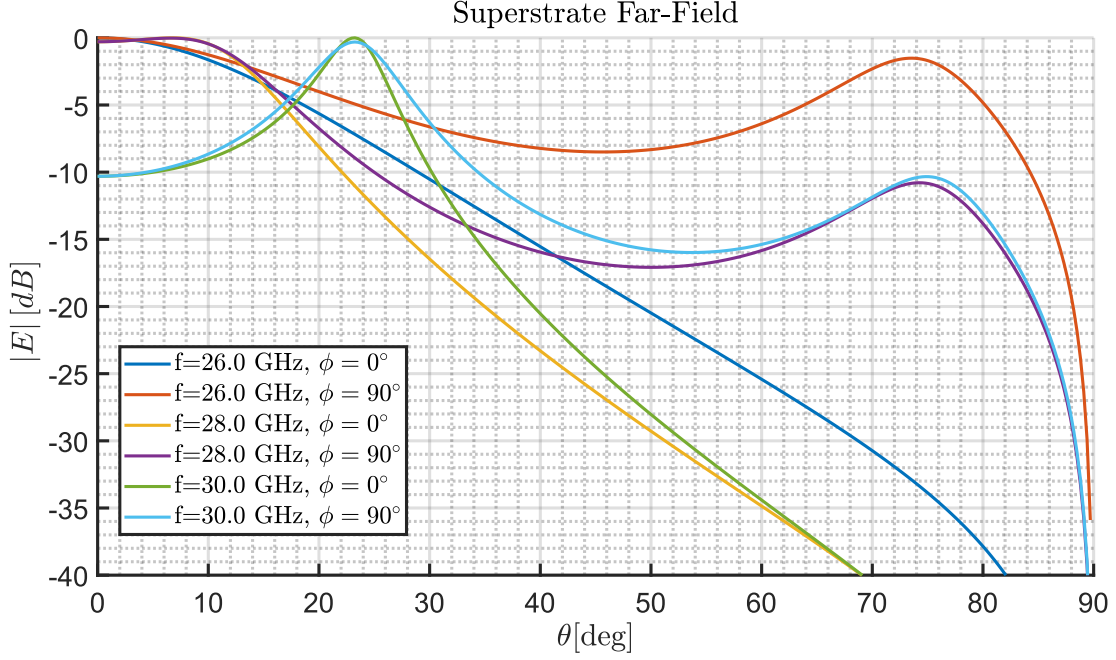


Figure 3: Farfield plot of superstrate geometry

The substrate thickness given by the following formula.

$$h_s = \frac{\lambda_0}{4\sqrt{\epsilon_r}} \quad (1)$$

The propagation constant of leaky wave modes is given by equation 2.

$$k_{plw} = \beta_{lw} - j\alpha_{lw} \quad (2)$$

where the real part of the propagation constant can be used to find the angle of the leaky-wave mode given by equation 3

$$\beta_{lw} = k_0 \sin \theta_{lw} \quad (3)$$

By analysing equation 3 one can see that at different frequencies the leaky-wave has different leaky-wave angles dependent on the real part of the propagation constant. Which is related to equation 4

$$\sqrt{\epsilon_r} \sin \theta_{lw} = \sin \theta_{lw0} \quad (4)$$

The saddle points at 26 GHz occur for TE at  $\theta = 74^\circ$  and for 28 GHz it occurs at  $75^\circ$  for TE. The saddle points occur at  $\theta = 23^\circ$  at 30 GHz for both TE and TM. where TE is when  $\phi = 90^\circ$  and TM when  $\phi = 0^\circ$ .

The bandwidth is given by the equation 5.

$$BW = 200 \frac{f_H - f_L}{f_H + f_L} \quad (5)$$

where  $f_H$  and  $f_L$  are the lower and higher frequencies at  $-3$  dB directivity. The Directivity plot for the superstrate geometry is given in the figure 5.

To obtain the bandwidth of the superstrate geometry the directivity for different permittivity values for the frequency range 9-11 GHz has been calculated and given in figure 4. From figure 5, one can observe that the bandwidth decreases with increasing  $\epsilon_r$  the reason for this can be explained by referring to the figure 4, as seen in figure 4 the directivity starts to peak around 9.95 GHz at the frequency mentioned the curve with  $\epsilon_r = 25$  directivity is maximum with 19.5 dB before and after the peak directivity decreases very fast for higher permittivities resulting in smaller bandwidths.

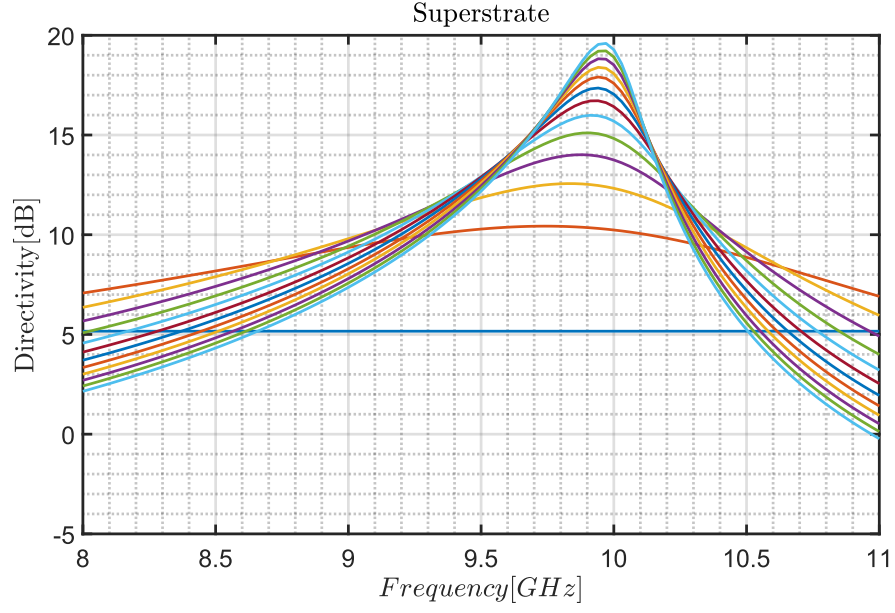


Figure 4: Directivity for different relative permittivity values, where directivity is lowest with 5 dB with  $\varepsilon_r = 1$  and highest for  $\varepsilon_r = 25$  with 19.5 dB

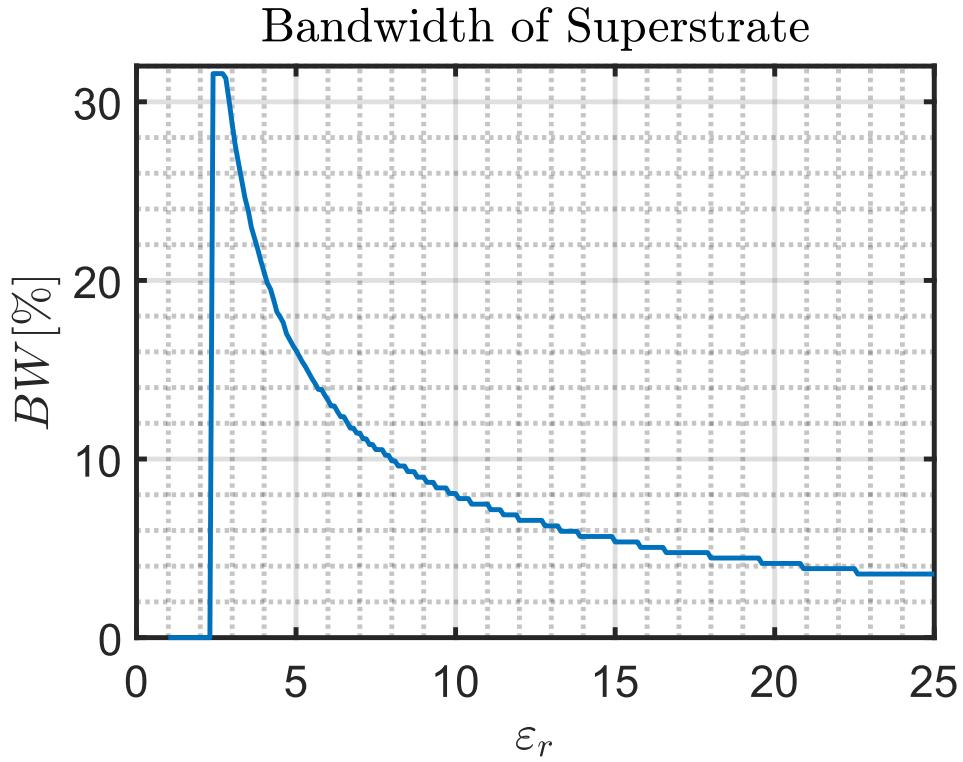


Figure 5: Bandwidth for different relative permittivity values

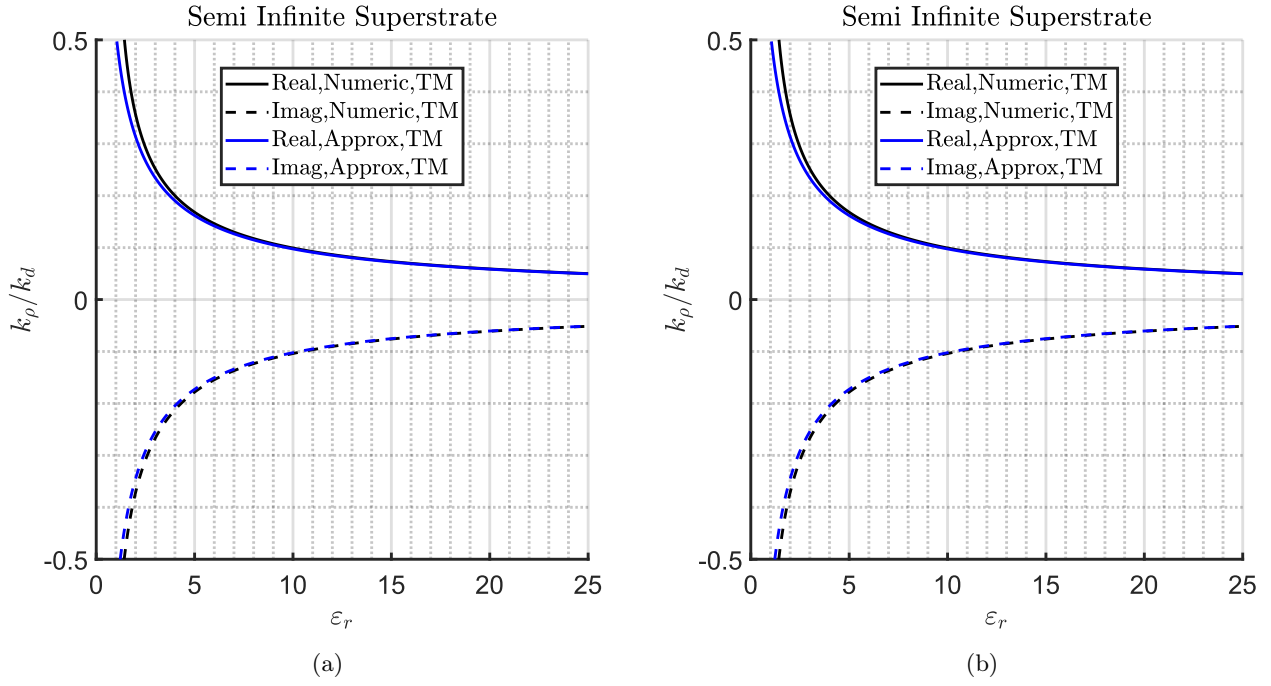


Figure 6: The change in propagation constant with relative permittivity (frequency=15 GHz), where 6a TM and 6b TE

## 2 Question 2: Semi-Infinite Superstrate Analysis

In this part of the assignment, a similar analysis to question 1 is done, where  $k_\rho$  for changing relative permittivity has been analysed at 15 GHz and plotted in 6. After that results of assignment 2 has been analysed.

The directivity plot for the semi-infinite superstrate structure is given in the figure ???. Similar to the previous question the directivity increases with increasing permittivity. However this time the directivity at permittivity equal to 25 is 6 dB higher.

From directivity calculated and using the equation 5 the bandwidth for the semi infinite superstrate has been calculated and given in the figure 8

As shown in the figure 8 the bandwidth is much larger at lower permittivities and much lower at higher permittivities. Compared to figure 5 one can see that overall bandwidth is higher for the semi-infinite superstrate.

The far-field plot of the semi-infinite superstrate structure is given in figure 9. The far-field is calculated at frequency 28 GHz,  $\epsilon = 12$  and air gap,  $h = 5.4$  mm.

As shown in the figure 9, saddle point occurs at  $\theta = 16.5^\circ$  in TE( $\phi = 90^\circ$ ) and there is no saddle point in TM( $\phi = 0^\circ$ ).

## 3 Question 3: Double Slot Fed Semi-Infinite Superstrate

Figure 10 shows the propagation constants for TM0 mode, apparently the frequency doesn't have any significant effect on the propagation constant of this mode.

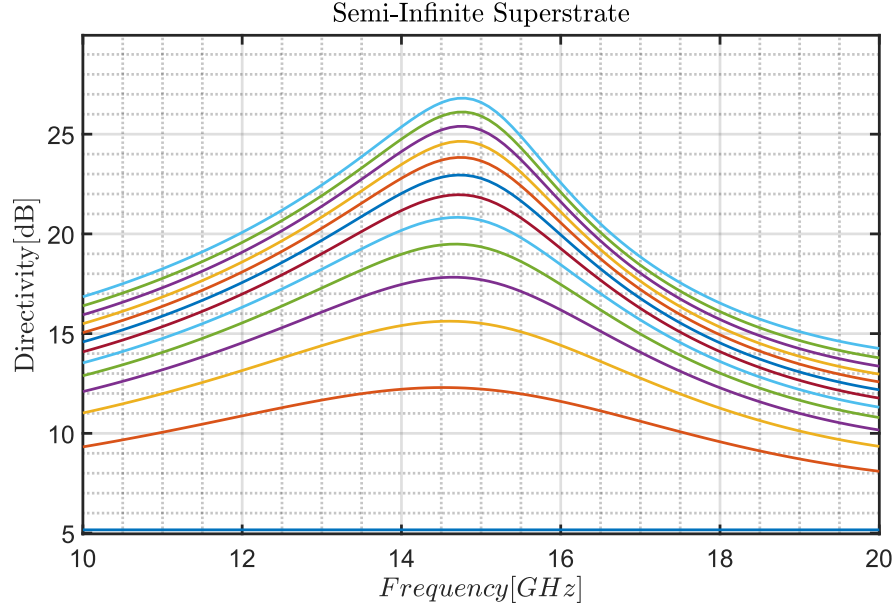


Figure 7: Changing directivity with frequency for different relative permittivity values. The directivity is lowest when the relative permittivity is 1 and highest when the relative permittivity is 25.

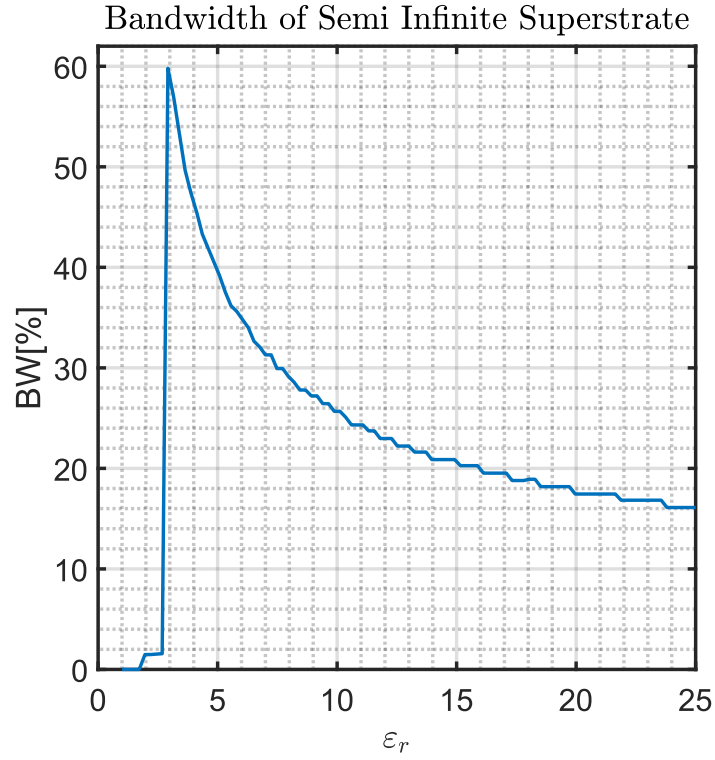


Figure 8: The bandwidth for semiinfinite superstrate structure

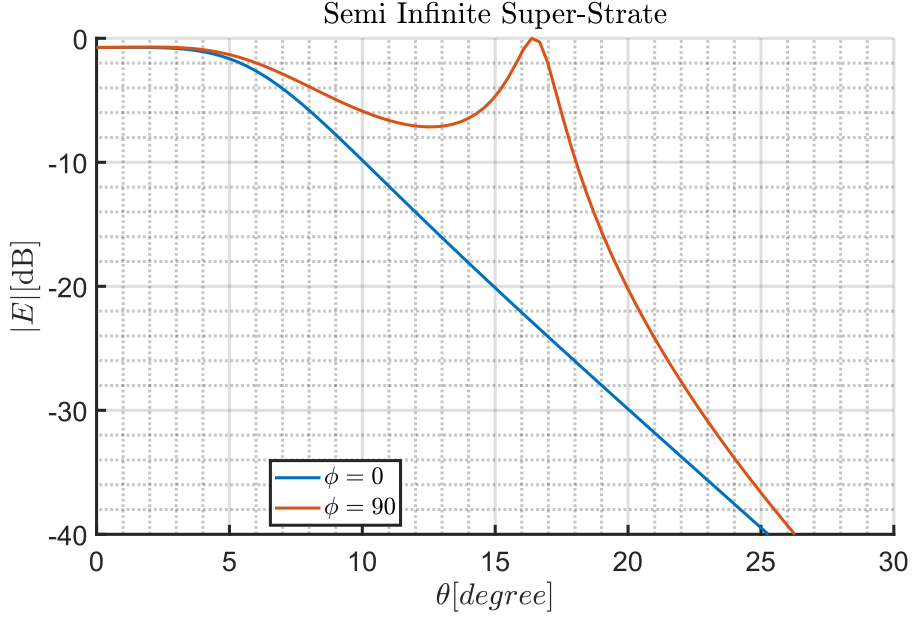


Figure 9: The far-field plot of the semi-infinite superstrate structure.

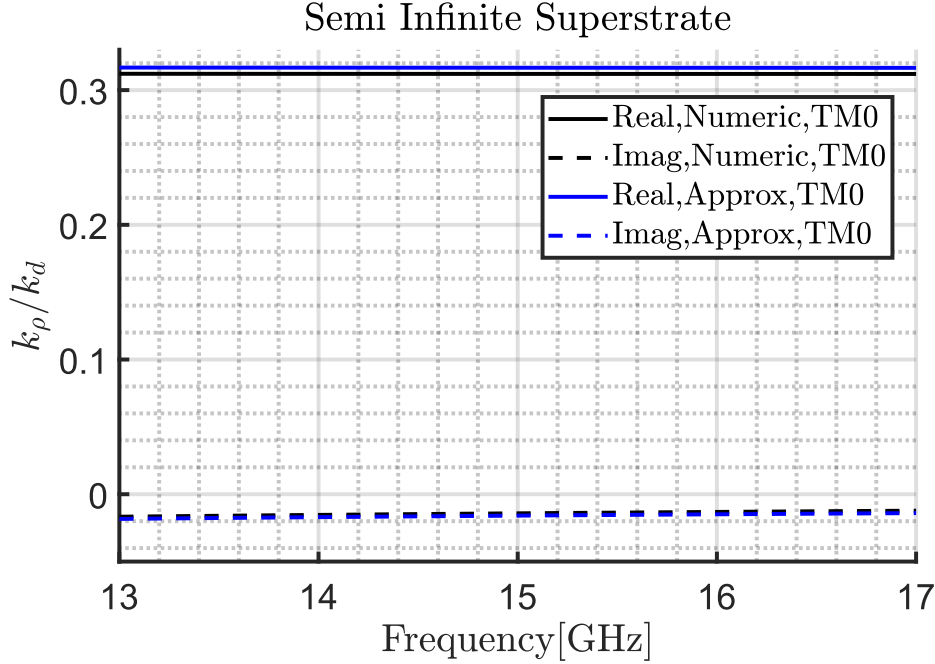


Figure 10:  $k_\rho$  of TM0 mode with increasing frequency

The optimum distance between the two slots can be calculated in a way to reduce the effect of leaky waves. From the figure  $k_{\rho lw}$  is  $(0.312 - j0.15)k_d$ . For  $\phi = 0^\circ$ ,  $k_{x, lw} = 0.312k_d$ . The wavelength of the leaky wave can be found as  $\lambda_{lw} = \frac{2\pi}{0.312k_d} = 1.014\lambda_0$ . To eliminate the surface waves the optimum separation between the slots is  $d = \lambda_{lw}/2 = 1.014\lambda_0/2$ .

Looking into the far-field plot of the single slot case saddle points are present at  $\theta = 20^\circ$ . This is also the case for the double slot case however for double slot the strength of the field at the saddle point is much less; the field strength at saddle point for the single slot is 0 dB at  $\phi = 0^\circ$  and -4 dB at  $\phi = 45^\circ$ , whereas for double slot there is only a saddle point with strength -10 dB at  $45^\circ$ . There is a null at  $\theta = 20^\circ$  at  $\phi = 0^\circ$  this can be a result of the array factor of the double slot.

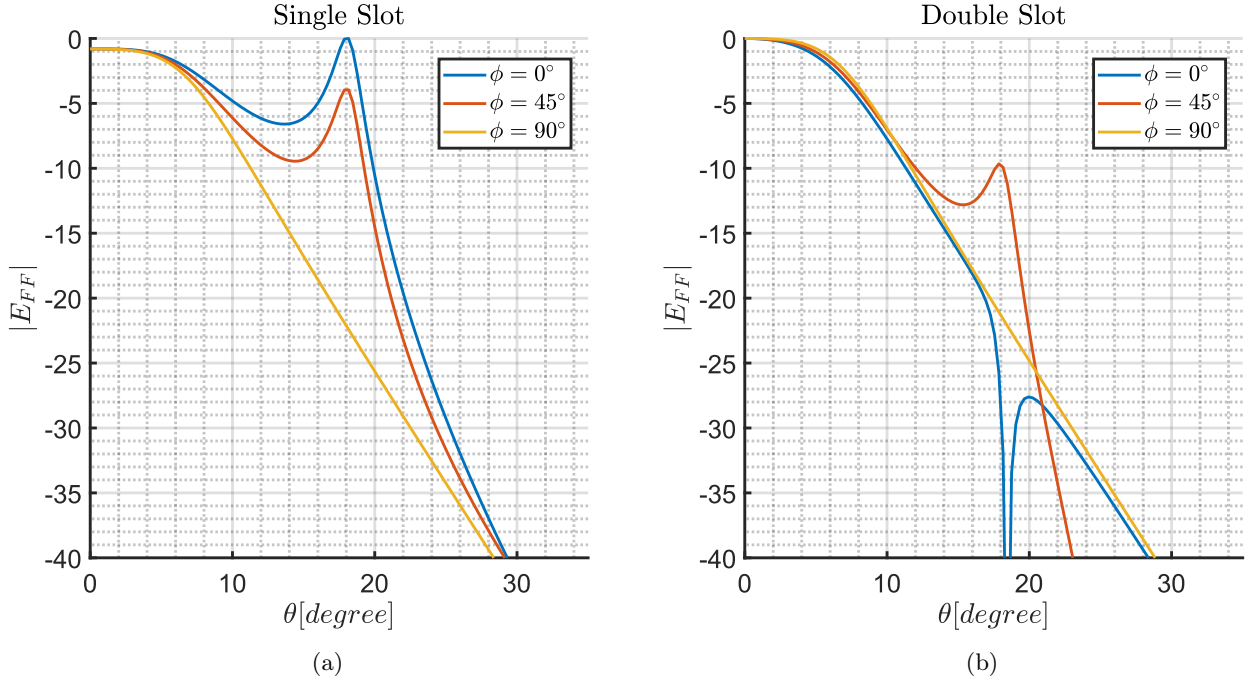


Figure 11: Far field plot of figure 11a single slot and figure 11b double slot.

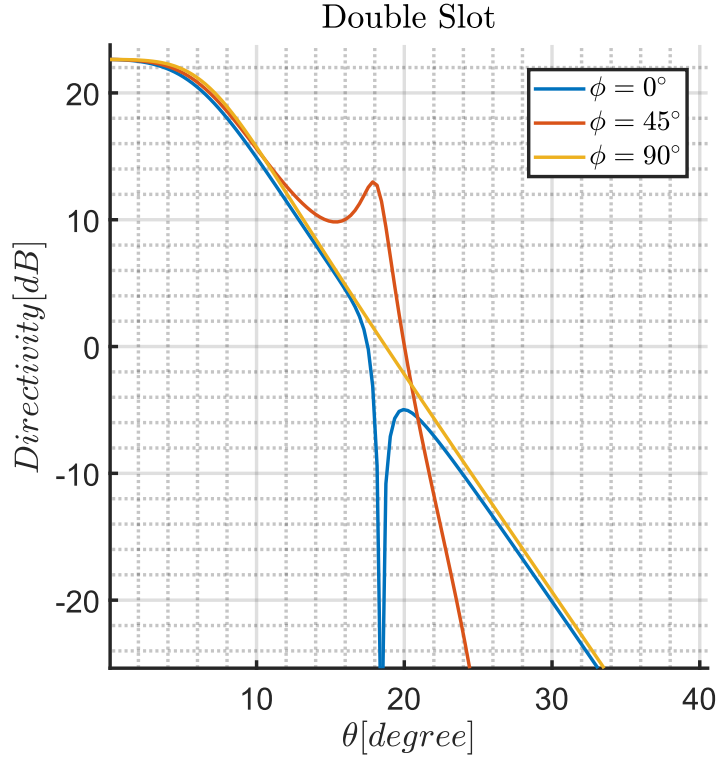


Figure 12: The directivity plot of the double slot fed semi-infinite structure.